



FACULTY OF SCIENCE

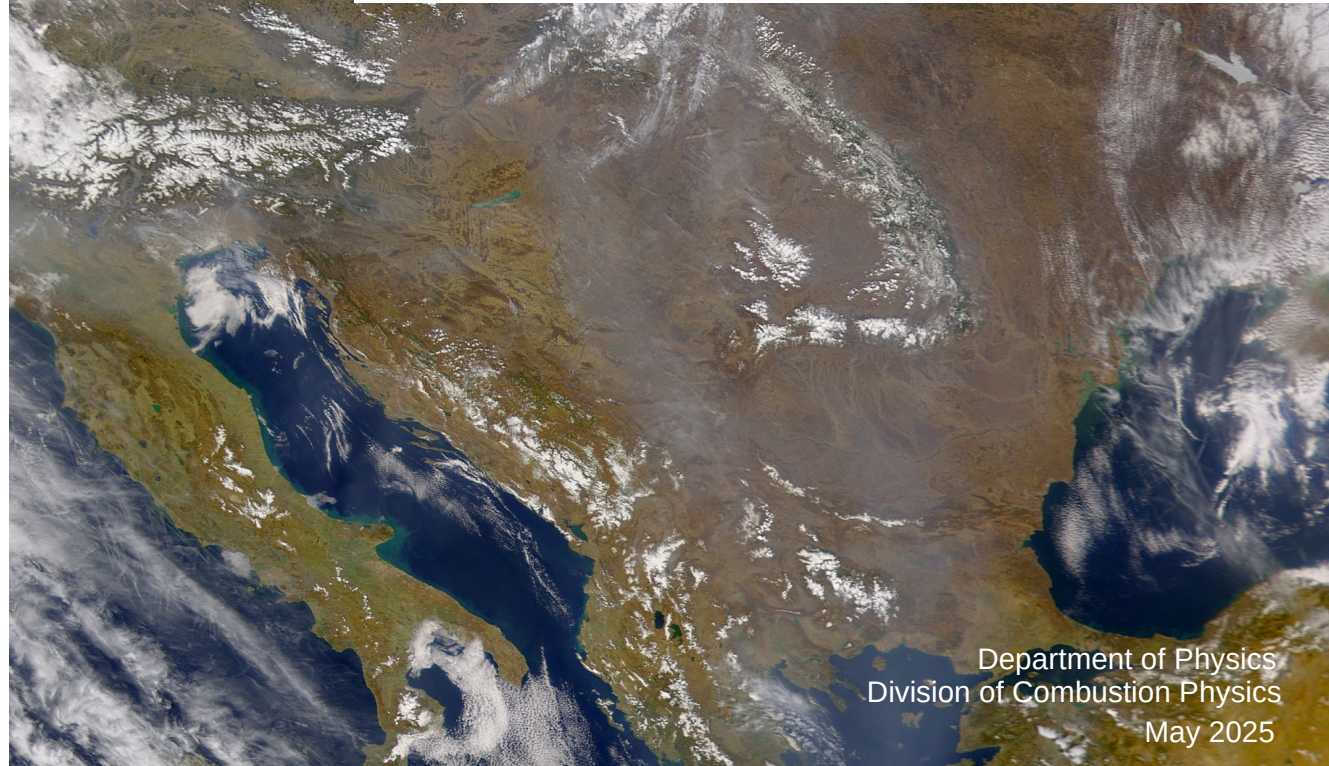


Relation Between High Pressure Blocking and Aerosol Concentrations in Southern Sweden

Fredrik Bergqvist

Thesis submitted for the degree of Bachelor of Science
Project duration: 2 months

Supervised by Moa Sporre



Department of Physics
Division of Combustion Physics
May 2025

Abstract

High-pressure blocking events are anticyclones that persist over a region for a long time. The event prevents vertical mixing of air pollutants due to the subsidence inversion created by the adiabatic compression of air during the anticyclone. This study investigated the relationship of aerosol concentrations during periods of high-pressure blocking events in southern Sweden for the rural location of Vavihill and the urban location of Malmö. A total of 247 high-pressure blocking events were found in Vavihill and Malmö between 1995 and 2024. The requirements for a high-pressure blocking event were: A pressure above 1014 hPa, the event lasting for at least 5 days, and having a maximum amount of rainfall of 0.5 mm h^{-1} . These criteria had to be fulfilled for the initial five days in both locations with a maximum time difference of 5 h. The PM_{2.5} levels during the progression of the high-pressure blocking events were compared to mean PM_{2.5} concentrations from the same location. The data was also sorted according to wind direction, season, and pressure strength for further analysis. Using Mann-Kendall statistics and standard deviations, the data showed a significant increase of PM_{2.5} for both locations during periods of high-pressure blocking. Higher PM_{2.5} concentrations were observed in Malmö due to larger local emissions, and a slightly stronger ground inversion. Peak aerosol levels were achieved after eight to thirteen days, indicating an accumulation of aerosols during the event in both locations. The investigation showed a stronger increase with winds from eastern and central Europe, indicating advective transport of aerosols to the region, although local emissions also played a significant role. This was supported by the findings of the seasonal and pressure strength dependencies, where stronger high-pressure blocking events showed the highest levels of PM_{2.5}. Although no increase in the frequency of high-pressure blocking events was found in the region, the impact on air quality from high-pressure blocking events is still crucial. These results show how aerosol concentrations depend on atmospheric events in the region.

Keywords: Aerosols, PM_{2.5}, high-pressure blocking, Mann-Kendall, southern Sweden, Skåne

Cover photo taken by SeaWiFS Project, NASA, on March 28 2003 [1].

Acknowledgments

Thank you, Moa Sporre, for your invaluable guidance throughout this thesis. One could not wish for a better supervisor. I would also like to thank Pub Rydberg for providing a pleasant weekly break during the writing of this thesis. Finally, thanks to my wonderful wife, Kastanja, for assisting with the text and proofreading the thesis.

Contents

1	Introduction	1
1.1	High-Pressure Systems	1
1.2	Aerosols	4
1.2.1	Aerosol Concentrations During High-Pressure Blocking Events	5
2	Method	6
2.1	The Data Handling and Devices	6
2.1.1	The Aerosol Data and Measurements	6
2.1.2	The Meteorological Data and Measurements	7
2.2	The Identification of High-Pressure Blocking Events	9
2.3	The Data Analysis	10
2.4	Statistical Evaluation: The Mann-Kendall Test and Sen's Slope	11
3	Results	12
3.1	The Change in Aerosol Concentrations	12
3.1.1	The Change in Aerosol Concentrations Depending on Wind Direction	14
3.1.2	The Change in Aerosol Concentrations Depending on Season	15
3.1.3	The Change in Aerosol Concentrations Depending on Pressure Strength	16
3.2	The Frequency of High-Pressure Blocking Events	18
4	Discussion	20
5	Conclusion and Summary	22
6	Outlook	22
A	Appendix: Access to Code	25

1 Introduction

It is common knowledge that Earth's increasing temperature has many side effects. One such effect is the increase in frequency of extreme weather phenomena [2]. One such phenomenon, which lacks extensive research, is high-pressure blocking events. A high-pressure blocking event is an anticyclone that covers an area for a prolonged period of time and often blocks other types of weather, hence the name. This results in limited cloud formations and a pronounced daily temperature variation [3]. However, an anticyclone is also associated with slower air movement, causing the air to remain stagnant. This can lead to an accumulation of air pollutants such as aerosols [4].

To investigate the relationship between aerosols and high-pressure blocking events, one must analyse periods of high-pressure blocking and examine the concentration of aerosols during these periods. Thus, the aim of this thesis is to: identify a suitable method for detecting periods of high-pressure blocking using pressure data from the *Swedish meteorological and hydrological institute* (SMHI); analyse these periods in relation to PM_{2.5} levels from rural (Vavihill, Svalöv, Skåne County) and urban (Malmö, Skåne County) areas. Additional relevant data, such as wind direction, season, and pressure strength will be examined to gain a comprehensive understanding of high-pressure blocking events and their characteristics. This thesis will also explore the frequency of high-pressure blocking events to determine whether this weather phenomenon is becoming more common, which is particularly important if a positive correlation with aerosol levels is found.

1.1 High-Pressure Systems

Anticyclones are meteorological high-pressure systems in which air sinks toward the ground, creating high pressure [5]. This occurs due to the convergence of air from all directions at high altitudes, which forces the air to move downward. The descending air undergoes adiabatic compression, resulting in an increase in the energy of the air molecules, or, in other words, a higher temperature. This rise in energy inhibits cloud formation, as warmer air can hold more moisture. The absence of clouds allows solar radiation to significantly impact the temperature during an anticyclone. Consequently, this leads to a large temperature difference between day and night, with summer anticyclones being associated with high temperatures and winter anticyclones with low temperatures.

Under normal conditions, the temperature of the air in the atmosphere decreases with the altitude, due to the adiabatic expansion of the air. The cooling per altitude is called the environmental lapse rate and makes it possible for vertical wind movement to occur, when a slight imbalance is introduced to the system. During an anticyclone, adiabatic compression of the air occurs as the air descends. This increases the temperature at lower altitudes. However, this downward movement of air does not reach the ground due to the friction opposed by buildings, forests, valleys, and other obstacles that create friction by disrupting the airflow. Thus, the downward draught will

spread out a few hundred meters above the ground and not mix with the air that lies closest to the ground. Since the air closest to the ground remains cool, while the air a few hundred meters up is warmer from the adiabatic compression, an inversion of the environmental lapse rate will be created. This process is called a subsidence inversion and will prevent air mixing between the ground level and the upper layers of the atmosphere [6]. The temperature profile due to the subsidence inversion can be seen in Figure 1.

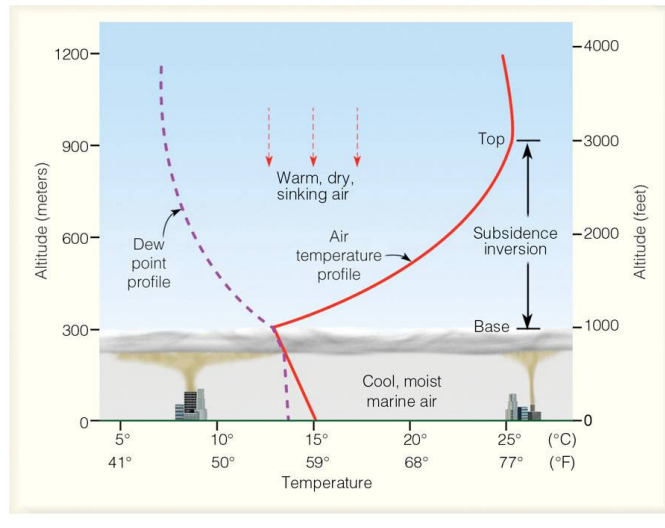


Figure 1: This figure shows how the temperature changes with altitude under a subsidence inversion in the atmosphere [7].

Another type of inversion occurs during the night as the air closer to the ground loses heat due to the outgoing radiation from the Earth. This process is especially strong due to the absence of clouds during the anticyclone. This creates a ground inversion layer, where the air temperature increases with height closer to the surface [8]. This ground inversion, created from the daily cycle, also prohibits vertical air movement in the atmosphere.

A high-pressure blocking period refers to a prolonged anticyclone characterized by higher surface pressure covering a large area [3]. Since the blocking event extends over a vast region, the pressure gradient remains small due to minimal fluctuations. As a result, the wind tends to be calm. A blocking period is typically defined as lasting between five and ten days, although some events can persist even longer [9]. However, no single definition of high-pressure blocking events exists [3]. An interesting observation is that the end of a high-pressure blocking event is followed by rainfall and or a strong shift in wind direction. While the concept has been recognized in meteorology for over a century, the long-term consequences of blocking events are not yet fully understood. High-pressure blocking periods are more common in the Northern Hemisphere compared to the Southern Hemisphere. Research has indicated that the frequency of blocking periods has increased in recent years [3].

Recurring anticyclones can be classified into Hess and Brezowsky macrocirculation types, such as the Fennoscandian High (HFA), the Southeast Anticyclone (SEA), and the Central European High (HM) [10]. HFA is centred on the Fennoscandinavian Peninsula (Norway, Sweden, Finland, and western parts of Russia) and is a recurring

anticyclone during the winter. This anticyclone is known for blocking air masses from the Atlantic, causing colder periods in the region. The SEA is a recurring anticyclone with its geographical center in southeastern Europe (the Balkans and western Türkiye). This anticyclone is most frequent during the summer months and is associated with heat waves. The HM is centred in central Europe (Germany, Poland, the Czech Republic) and occurs during both the summer and winter months. The center of these anticyclones can be seen in Figure 2.

To explain the air movement during an anticyclone the Navier-Stokes equation can be used,

$$\frac{\partial \vec{v}}{\partial t} + (\vec{v} \cdot \nabla) \vec{v} = \vec{g} - \frac{\nabla p}{\rho} - 2(\vec{\Omega} \times \vec{v}). \quad (1)$$

The first term in the Navier-Stokes equation corresponds to the local acceleration of the air, the second term corresponds to the convective acceleration of the air, the third term is simply the gravitational acceleration, the fourth term describes the force from the pressure gradient and the last term describes the Coriolis force. Since the aim is to examine the stable solution of this equation, we can assume that the local acceleration is zero. The weather system is a large scale system with the size of hundreds of kilometres, the speed is in the tens of meters per second and the Coriolis term is in the order of $0.5 \times 10^{-4} \text{ s}^{-1}$. Using this information one can observe that the size of the convection term is negligible in comparison to the Coriolis term. Lastly, one can assume the wind to be in the horizontal plane since vertical movement is a lot slower, providing a definition of the wind vector as $\vec{v} = (v_x, v_y, 0)$. The Coriolis term can be approximated by considering only the vertical component as $\vec{\Omega} = (0, 0, \Omega_z)$, since the horizontal components are negligible and Earth's rotation primarily projects along the vertical axis, causing deflections in the horizontal plane. The Navier-Stokes equation is thus simplified in the case of a stable large scale weather systems to

$$0 = -\frac{\nabla p}{\rho} - 2\vec{\Omega} \times \vec{v}, \quad (2)$$

where the gravity is neglected since it lies in the vertical plane while the wind lies in the horizontal plane. Solving for the horizontal velocity components from this equation one obtains the solution

$$v_x = -\frac{1}{2\rho\Omega_z} \frac{\partial p}{\partial y} \text{ and } v_y = \frac{1}{2\rho\Omega_z} \frac{\partial p}{\partial x}. \quad (3)$$

Examining the vorticity of the horizontal wind, one obtains

$$(\nabla \times \vec{v})_z = \frac{1}{2\Omega_z \rho} \nabla^2 p, \quad (4)$$

where the definition of the anticyclone (the pressure is strongest in the center) implies that $\nabla^2 p$ is negative. Since $\nabla^2 p$ is negative the vorticity is also negative, implying that the anticyclone rotates clockwise in the Northern Hemisphere. Since anticyclones exhibit winds rotating clockwise around their center, the winds from HFA, SEA, and HM tend to blow toward southern Sweden from the south, east and west, as can be seen in Figure 2. The transport of airborne pollutants, such as ozone, can occur via these winds [11]. Consequently, it can be hypothesized that other airborne aerosols, such as PM_{2.5}, should also be transported through these wind patterns.

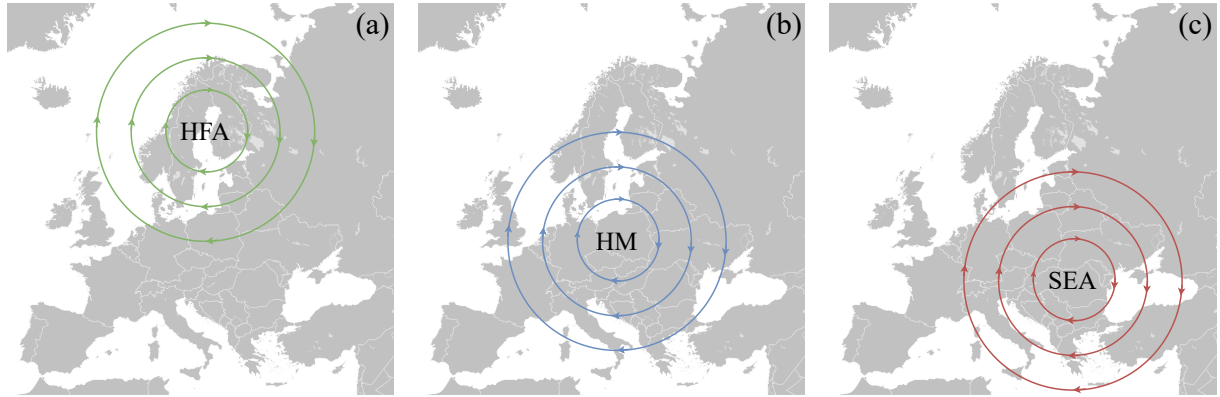


Figure 2: These maps show the air movement during the HFA, HM, and SEA blocking events [12]. The figures only show the general streamlines of the Brezowsky macrocirculation types, meaning that the real world anticyclones would not be perfectly circular.

1.2 Aerosols

Aerosols are liquid or solid particles suspended in the air. The concentration of aerosols in the air can be measured by the combined mass of the particulate matter per volume. However, it is important to specify which types of particles are being measured, where PM_{2.5} (particulate matter with an aerodynamic diameter of 2.5 µm or less) is a common choice because PM_{2.5} is easy to measure. Furthermore PM_{2.5}, like any other aerosol, impacts the health significantly and is able to be transported by the wind. Although aerosols can form naturally in the atmosphere, the primary sources in urban and suburban Europe include solid fuel combustion for domestic heating, industrial activities, and road transportation [13]. Particulate contributors to PM_{2.5} include sulphur dioxide (SO₂) and soot (black carbon), both originating from the burning of fossil fuels. The European Union set an annual mean limit for PM_{2.5} concentrations at 25 µg m⁻³ in 2008, although the WHO suggested a much lower threshold of only 5 µg m⁻³ [13]. In 2022, the EU mean limit threshold was exceeded in several countries, including Croatia, Bosnia and Herzegovina, Italy, Poland, North Macedonia, and Türkiye [13].

Studies have demonstrated a correlation between elevated PM_{2.5} concentrations and an increased risk of respiratory, cardiovascular, and cerebrovascular diseases, as well as diabetes [14]. A Danish study on 49 564 individuals between 1993 and 2015 showed that for every 5 µg m⁻³ increase in aerosol concentrations the hazard ratio increased by 1.29 [15]. Thus, for every 5 µg m⁻³ increase in PM_{2.5} the risk of dying from cardiovascular diseases increased by 29 %. Further studies on PM₁₀, which is closely related to PM_{2.5}, showed that in the age group of 75-84 mortality increased 36 % and 106 % in the age group 85+ during health waves associated with high PM₁₀ concentrations [16].

1.2.1 Aerosol Concentrations During High-Pressure Blocking Events

During a high-pressure blocking event the environmental lapse inversion, especially the subsidence inversion, close to the ground prohibits vertical air mixing during the atmospheric layers closest to the ground. If aerosols are produced at ground level during this high-pressure blocking event, this would imply that the aerosols would not disperse vertically, implying a higher concentration on the ground level. Thus, one would expect higher concentrations of PM_{2.5} during high-pressure blocking events. Chinese studies have shown that the vertical dispersion of aerosols during high-pressure blocking events are inhibited, increasing the concentration of PM_{2.5} in cities [4].

Since aerosol emissions are particularly high in central European countries such as Poland, anticyclonic winds from the south and east from HFA, SEA, and HM are expected to increase PM_{2.5} concentrations in southern Sweden [13]. These aerosols would be transported to southern Sweden via southerly to easterly winds during the anticyclone, Figure 2. If this occurs during a high-pressure blocking event, the aerosols may accumulate over the region while continuously being advected by southerly and easterly winds. A schematic figure showing why aerosols levels should increase in southern Sweden under high-pressure blocking events can be seen in Figure 3.

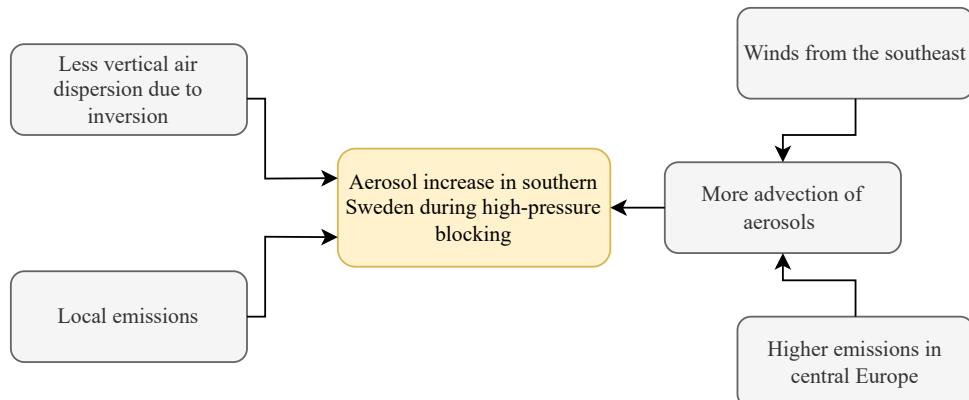


Figure 3: This figure show why an aerosol increase should be observed during high-pressure blocking events in southern Sweden.

2 Method

2.1 The Data Handling and Devices

The meteorological data was downloaded from the SMHI's website as CSV files. The data included hourly atmospheric pressure data, hourly rain data, and hourly wind data (speed and direction). Hourly aerosol data as PM_{2.5}, measured over one-hour intervals, was also downloaded. Since the purpose of this thesis was to analyse aerosol concentrations in southern Sweden during high-pressure blocking events, one urban and one rural site were selected. The locations were chosen based on their classification as rural or urban and the length of time the stations had been in operation, where more data was considered better.

2.1.1 The Aerosol Data and Measurements

The rural measuring station in the county of Skåne with the most aerosol data was Vavihill located in Svalöv, southern Sweden. This station was active from September 28, 1999, to November 15, 2017. However, due to missing data on some days, only 57 % of the period contained non-missing values. Additionally, between 2017 and 2018, the Vavihill station was relocated to nearby Hallahus, where it operated from May 10, 2018, to December 31, 2022, with 93 % of the period containing non-missing values. Combining these datasets resulted in a total of 5371 days of hourly data. For an urban location in the county of Skåne, Malmö Rådhuset had the most data, with measurements recorded from June 3, 1999, to December 31, 2023. Here, 90 % of the recorded values were non-missing, resulting in 8074 days of data. The geographical location of the two locations, together with pictures showing the surrounding area, can be seen in Figure 4.

The measurement device used at Vavihill was the ambient particulate monitor TEOM 1400. This monitor continuously collects airborne particles less than 2.5 µm onto a filter and measures their mass using an oscillating microbalance technique [17]. The oscillating microbalance works by vibrating at a natural frequency, which changes as particles accumulate on the filter. Since this frequency shift is proportional to the mass of the particles, their total mass can be calculated. The precision of the monitor was $\pm 1.5 \mu\text{g m}^{-3}$. Thus, the monitor provides high precision and stable measurements. However, a key limitation is that it cannot distinguish between different types of particles, as it only measures total mass. When the measuring station was moved to Hallahus, the measuring device was updated to the fine dust analysis system Palas FIDAS 200. This device works by an optical aerosol spectrometer, which samples particles from an isokinetic inlet through a polychromatic light-scattering channel where the scattering angles and intensities are measured. [18]. This results in a high accuracy of $\pm 0.1 \mu\text{g m}^{-3}$, indicating an improvement from the previous device.

The monitoring station in Malmö used several measuring devices over time, in conjunction with other equipment. Between the start of the monitoring and January 1, 2009, the TEOM 1400 monitor was used. From January 1, 2009, to December 31, 2015, the TEOM 1400, FDMS, and 8500 B or CB dryer were employed. Between January 1, 2016, and December 31, 2021, the TEOM 1405F and FDMS systems, along with the 8500 B, were in use. Finally, from January 1, 2022, the Palas FIDAS 200 monitor replaced the earlier systems. The FDMS (Filter Dynamics Measurement System) is a dynamic filter measurement system that enhances measurements by accounting for volatile and semi-volatile particles [19]. The CB dryer and 8500 B are air dryers used to prevent moisture from entering the measurement devices, ensuring accurate data by avoiding interference caused by water vapour.

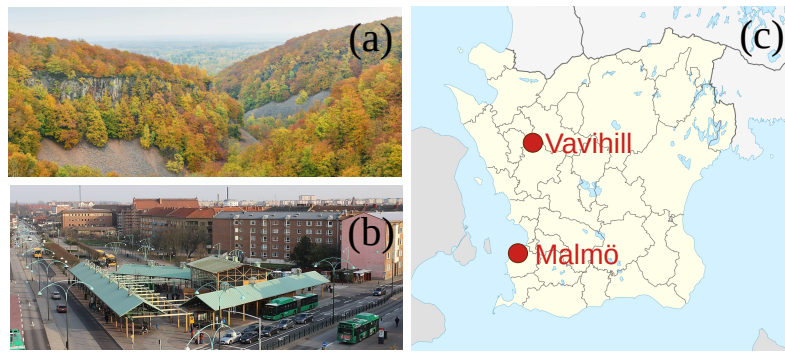


Figure 4: Pictures showing (a) the nearby national park, Söderåsen, to Vavihill [20], (b) a bus station in Malmö [21], and (c) a map displaying the locations [22].

2.1.2 The Meteorological Data and Measurements

The meteorological data which was used in this thesis can be observed in Table 1. The time periods listed in the table show which periods was used this study, which may not represent the full operational range of the stations. Note that no particle data was collected from Ängelholm since this station was only used for detecting high-pressure blocking event during the last 74 years. The reason for not displaying wind data for Ängelholm was simply due to none being available for this location. Also, the absence of device information in Ängelholm is due to airport security restrictions. Overall, the choice of locations was based on the proximity to the PM_{2.5} measuring stations in the case for Vavihill and Malmö, and in the case of Ängelholm due to its proximity to the pressure measuring station. For Vavihill the wind and rain station had to be non coastal, since Vavihill is non coastal. This is because coastal regions can experience a daily cycles of sea breezes and land breezes, which alter the wind direction. Given that Ängelholm is situated 44 km from Vavihill and 76 km from Malmö, it is reasonable to question whether atmospheric pressure varies significantly over these distances. However, during the period from December 1, 1995, to October 1, 2024, the mean difference in pressure between Ängelholm and Helsingborg was (0.25 ± 0.20) hPa, indicating minimal change.

The PTB201A digital barometer operates using a silicon capacitive absolute pressure sensor, providing stable and accurate pressure values [23]. The sensor functions by means of a flexed diaphragm inside a capacitor that bends in

response to air pressure, causing a change in the capacitor's distance and thus a variation in the current. This device measures pressure in the range of 600 hPa to 1100 hPa, with an accuracy of ± 0.3 hPa. Errors in the device may arise due to environmental factors, such as exposure to condensing gases. The Vaisala PTB220 digital barometer operates in a similar manner but offers a wider measurement range of 500 hPa to 1100 hPa, with an improved accuracy of ± 0.15 hPa [24]. The barometers used had been serviced every year or every other year.

The WAA15A anemometer works by a rotating chopper disc that interrupts an infrared beam, resulting in a laser pulse proportional to the wind speed [25]. The WAV15A wind vane uses a counterbalanced vane with an optical disc. When the vane turns, infrared LEDs detect the change in angle with the disc and phototransistors, resulting in a precise measurement of the wind angle. The WAA15A anemometer measured wind speed with an accuracy of $\pm 0.17 \text{ ms}^{-1}$, and the WAV15A wind vane measured the wind direction with an accuracy better than $\pm 3^\circ$. The wind instruments were serviced and calibrated every year or every other year, and had been in use since 1995. Like the wind monitor, the Geonor T200 rain monitor had been serviced and calibrated every year or every other year. This device works by measuring precipitation with a vibrating wire sensor that detects weight changes from the water droplets [26]. The device has a measurement accuracy better than $\pm 0.1 \text{ mm}$.

Table 1: The meteorological data for each location.

		Vavihill	Malmö	Ängelholm
Air pressure	Station	Helsingborg (25 km away from particle monitor)	Helsingborg (49 km away from particle monitor)	Ängelholm airport
	Period	August 2, 1995 to October 10, 2024.	August 2, 1995 to October 10, 2024.	January 5, 1946 to October 1, 2024
	Device	Vaisala PTB220 (April 15, 2015, to April 17, 2025, and from September 19, 2004, to May 23, 2014) PTB201A (Remaining time)	Vaisala PTB220 (April 15, 2015, to April 17, 2025, and from September 19, 2004, to May 23, 2014) PTB201A (Remaining time)	No info
Wind	Station	Hörby (35 km away from particle monitor)	Malmö (6 km away from particle monitor)	-
	Period	August 1, 1995, to October 1, 2020.	January 1, 1990, to December 31 2020.	-
	Device	Vaisala WAA15A (speed) Vaisala WAV15A (direction)	Vaisala WAA15A (speed) Vaisala WAV15A (direction)	-
Rain	Station	Hörby (35 km away from particle monitor)	Malmö (6 km away from particle monitor)	Ängelholm and Tånga.
	Period	August 1, 1995, to October 1, 2020.	November 21, 1995, to December 31 2020.	January 18, 1947, to November 30, 2001 and December 19, 1973 to August 31, 2024.
	Device	Geonor T200	Geonor T200	No info and beaker.

2.2 The Identification of High-Pressure Blocking Events

To evaluate the occurrence of high-pressure blocking event for Vavihill or Malmö, the rain data and atmospheric air pressure were used, which can be seen in Figure 5. For a period to be defined as a high-pressure event, the atmospheric pressure had to be over 1014 hPa, and the rainfall had to be less than 0.5 mm h^{-1} . These values were based on the fact that 1014 hPa was the mean atmospheric pressure from Helsingborg, and 0.5 mm h^{-1} was chosen since this is considered as very light rain. Since a high-pressure blocking event covers a large geographical area, and Vavihill and Malmö are located close to each other, a blocking event observed at one location should also be detectable at the other. To account for this, all identified high-pressure blocking events at one location were required to correspond to an event at the other location within a maximum time difference of 5 h. However since Vavihill and Malmö used the same air pressure measuring station, this meant that the precipitation in both locations had to be under 0.5 mm h^{-1} for the event. For a high-pressure event to be considered a high-pressure blocking event, the criteria for a high-pressure event had to persist for at least 120 h (5 days). This value was chosen since a 5-day limit is often considered when classifying high-pressure blocking events [3].

The rain-limit was set to 2 mm d^{-1} in Ängelholm since daily precipitation measured used instead. This value was chosen since it corresponds to a small amount of rainfall for a day, and almost no rainfall should be observed during high-pressure blocking events. The choice of 0.5 mm h^{-1} for hourly data is motivated by the fact that continuous light rain over a 24-hour period is very rare. As a result, daily precipitation levels seldom reach 12 mm d^{-1} , and are more commonly around 2 mm d^{-1} .

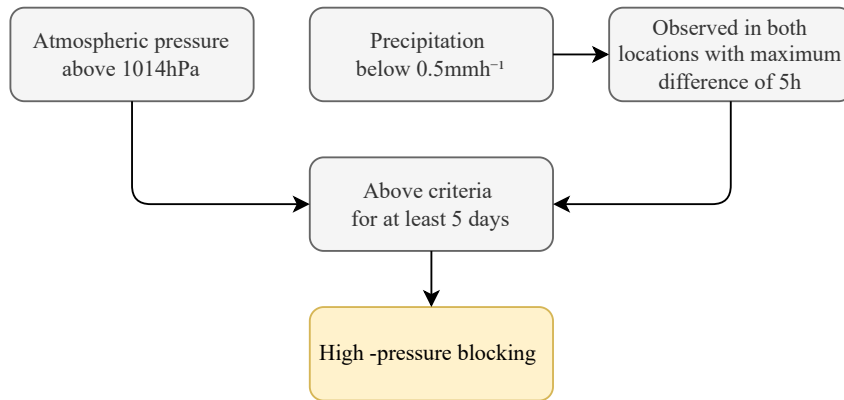


Figure 5: This figure show how a high-pressure blocking events was defined in Vavihill and Malmö.

2.3 The Data Analysis

The evolution of PM_{2.5} during the high-pressure blocking events were evaluated by calculating the mean and standard deviation of PM_{2.5} for each hour of all the high-pressure blocking events, to evaluate the average progression of aerosols over time. This was done using the Python packages NumPy and pandas. Since the high-pressure blocking events varied in length, a minimum of eight events was required when calculating the mean and standard deviation on the PM_{2.5} data. The mean PM_{2.5} value was then compared with the mean PM_{2.5} value during periods without high-pressure blocking events, as well as with the EU annual mean limit for PM_{2.5}. Due to the lack of PM_{2.5} data during some high-pressure blocking events, a filter was applied, stating that a period needed 85 % PM_{2.5} coverage in order to be analysed.

To evaluate if the PM_{2.5} levels returned to normal after the end of the events, the mean and standard deviation were also calculated from the end onwards. This clarified whether an increase was observed and whether it corresponded to the high-pressure blocking event or not. Furthermore, if elevated levels were observed, this helped evaluate how quickly the levels returned to normal.

The data was sorted in different ways to explore how the PM_{2.5} concentration depended on different parameters. Firstly, the data was sorted into one of four wind categories: northeast (310° to 70°), southeast (70° to 190°), west (190° to 310°), and no specific direction. This was done by categorizing the data if 60 % of the wind directional data fell into one of these categories, with zero wind speed being handled as a missing value.

Secondly, the data was sorted based on the season of the blocking. This was evaluated by taking the midpoint date of the blocking and categorizing the season by the month it occupied. December, January, and February were considered winter; March, April, and May were considered spring; June, July, and August were considered summer and September, October, and November were considered autumn. Lastly, the data was categorized based on the strength of the high-pressure blocking, where a weak high-pressure blocking event had a mean atmospheric pressure between 1014 hPa and 1020 hPa, a medium strong event had a mean atmospheric pressure between 1020 hPa and 1025 hPa, and a stronger event had a mean atmospheric pressure over 1025 hPa.

The last task of this study was to evaluate whether high-pressure blocking events had become increasingly more common. This was evaluated in two different ways: by calculating the number of days under high-pressure blocking events per year, and the number and lengths of high-pressure blocking events per year. The number of days of blocking was also sorted by the season of the blocking to provide more insight into the nature of the high-pressure blocking events.

2.4 Statistical Evaluation: The Mann-Kendall Test and Sen's Slope

To evaluate statistical significance of the trends found in the study, the statistical Mann-Kendall test was used. The Mann-Kendall test was applied to evaluate whether the PM_{2.5} mean during high-pressure blocking events had increased, and if so, by how much. The Mann-Kendall test is a non-parametric statistical test used to calculate the monotonic trend and the significance of the result of a dataset. This test is commonly used in climate physics due to the challenges posed by many parameters and complex distributions. The test works by calculating the difference between each time step in the dataset. The output will be a p-value below 0.05 if the test provides a significant result, meaning that the trend is unlikely to be caused by randomness. Kendall's τ -value is used to evaluate the monotonic increase of the dataset, where -1 indicates a total monotonic decrease, 1 indicates a total monotonic increase, and 0 indicates no monotonic trend. The τ -value can be summarized by the formula

$$\tau = \frac{C - D}{C + D}, \quad (5)$$

where C is the number of concordant pairs and D is the number of discordant pairs. A Concordant pair is when two neighbouring data points increase with the time step, and discordant pair decreases with the time step. If the result yielded a τ -value above 0.5, the result was labelled as a clear increase.

Sen's slope is a method, often used together with the Mann-Kendall test, of performing linear regression on the data. If a monotonic increase is shown by the Mann-Kendall τ , Sen's slope provides an estimate of the magnitude of that increase. The method differs from the least squares method because it uses the median to calculate the slope. This ensures that outliers, which are common in weather data, do not affect the results. Sen's slope is calculated as

$$S_i = \frac{\rho_{i+1} - \rho_i}{t_{i+1} - t_i} \quad \text{Sen's slope} = \text{median}(S_i), \quad (6)$$

where i represents the indices, ρ represents the concentration of PM_{2.5}, and t represents time. The program used for the Mann-Kendall test was the `pymannkendall` package in Python [27].

3 Results

3.1 The Change in Aerosol Concentrations

After applying the high-pressure blocking detection method to the data from Vavihill and Malmö for the entire period, a total of 213 high-pressure blocking events were identified between November 27, 1995 and September 22, 2024. For Vavihill 114 high-pressure blocking events of the original 213 were removed due to insufficient PM_{2.5} data, as a filter requiring 85% data coverage was applied. This left 99 relevant high-pressure blocking events. For Malmö 48 high-pressure blocking events were removed due to insufficient PM_{2.5} data, again applying the 85% data coverage filter. This resulted in 165 relevant high-pressure blocking events. An example plot showing periods of high-pressure blocking events can be seen in Figure 6. This figure provides insight into the categorization of high-pressure blocking events for the two different locations.

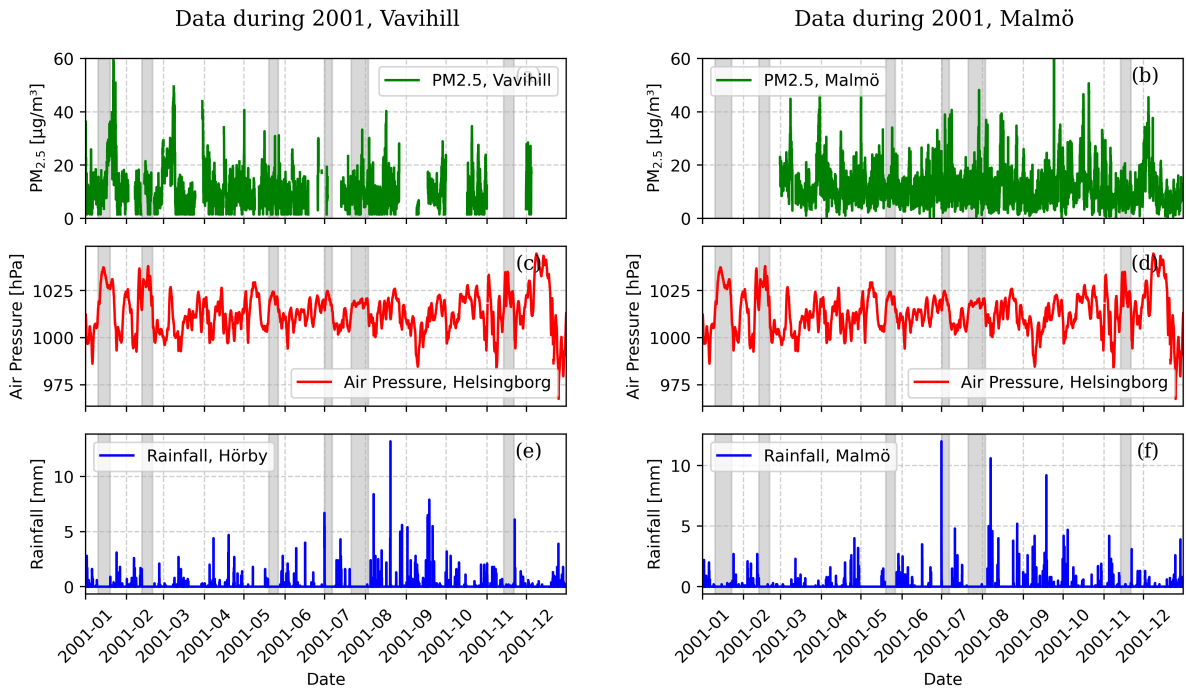


Figure 6: Example plots displaying the air pressure, PM_{2.5} concentrations, and rainfall during the year 2001. The periods which were indicated as periods of high-pressure blocking events are shaded in gray. This displays a normal yearly distribution of high-pressure blocking events using the described method.

The average change in PM_{2.5} concentrations during periods of high-pressure blocking can be seen in Figure 7. The data is compared with the PM_{2.5} mean taken from periods without high-pressure blocking events. An increase in PM_{2.5} concentrations can be seen in Malmö from 10 µg m⁻³ to a maximum of 21 µg m⁻³ at day thirteen, and an increase from 7 µg m⁻³ to a maximum of 18 µg m⁻³ at day twelve can be seen in Vavihill. The increase is supported

by the large τ -value of $\tau = 0.78$ in Malmö, and slight lower $\tau = 0.70$ in Vavihill. The Sen's slope values also indicate a stronger increase in Malmö $3.0 \times 10^{-2} \mu\text{g m}^{-3} \text{d}^{-1}$ compared to $2.1 \times 10^{-2} \mu\text{g m}^{-3} \text{d}^{-1}$ in Vavihill. After the first five days, the number of high-pressure blocking events decreases, which is reflected in the increase in standard deviation.

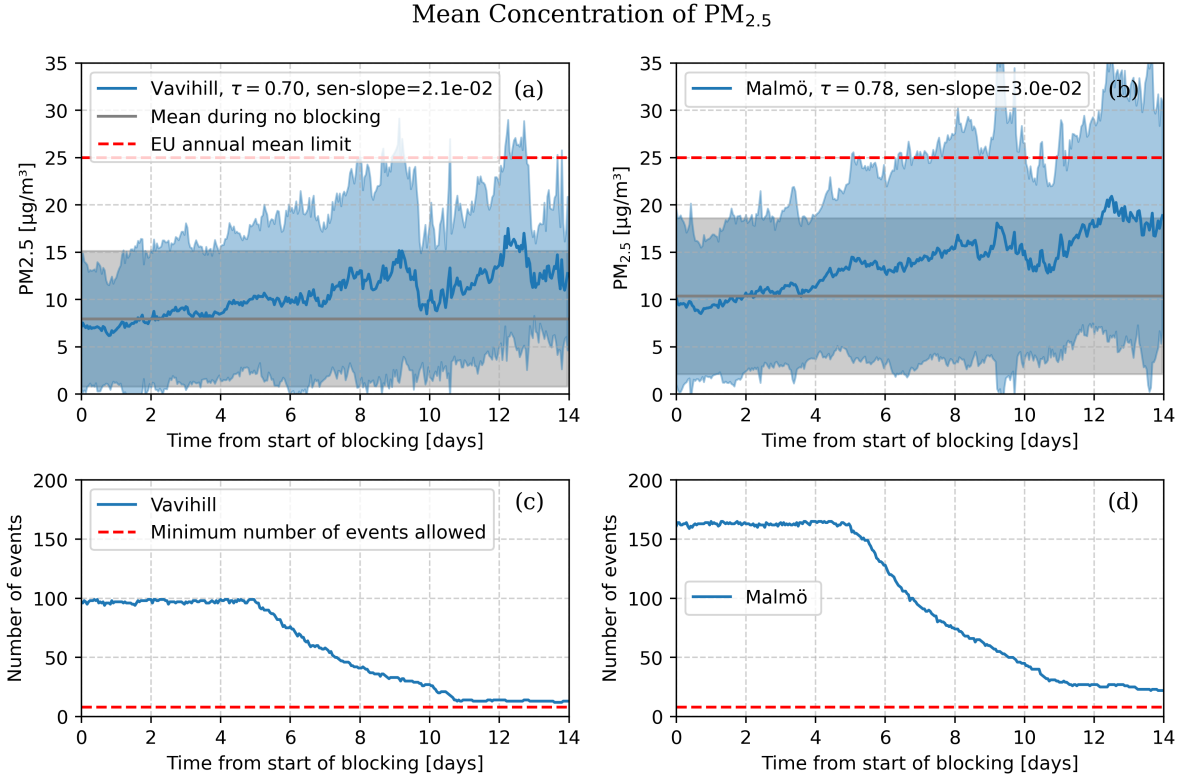


Figure 7: Mean $\text{PM}_{2.5}$ concentrations in Vavihill (a) and Malmö (b) during high-pressure blocking events (blue line). The grey line shows the mean $\text{PM}_{2.5}$ during non-high pressure blocking events. The shaded region indicates the standard deviation of the data. The number of high-pressure blocking events used in the analysis can be seen in (c) and (d), where the minimum number of events allowed was shown by the red line.

The average change in $\text{PM}_{2.5}$ concentrations after periods of high-pressure blocking can be seen in Figure 8. Observing this plot one can observe that after the end of a high-pressure blocking event the $\text{PM}_{2.5}$ levels return to normal during the first day after the end of the event. This is an interesting result which highlights that the increase observed in Figure 7, is indeed due to the presence of a high-pressure blocking event. This behaviour should be expected since high-pressure blocking event often end in rainfall, or change of wind direction which would contribute to a fast decrease in aerosols concentrations.

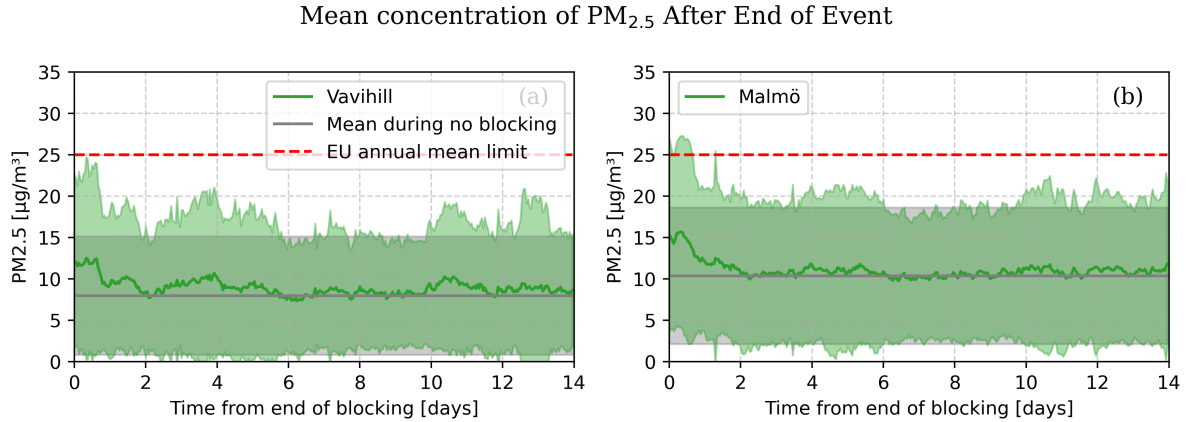


Figure 8: Mean $\text{PM}_{2.5}$ concentrations in Vävihill (a) and Malmö (b) after the end of high-pressure blocking events (green line). The grey line shows the mean $\text{PM}_{2.5}$ during non-high pressure blocking events. The shaded region indicates the standard deviation of the data.

3.1.1 The Change in Aerosol Concentrations Depending on Wind Direction

The change in $\text{PM}_{2.5}$ concentrations in Vävihill and Malmö during high-pressure blocking events for different wind directions can be seen in Figure 9. In the case of Vävihill, 7.1% of the winds came from the northeast (310° to 70°), 27.3% from the southeast (70° to 190°), 23.2% from the west (190° to 310°) and 42.4% from no specific direction. In the case of Malmö, 7.9% of the winds came from the northeast (310° to 70°), 24.8% from the southeast (70° to 190°), 18.2% from the west (190° to 310°) and 49.1% from no specific direction. Very little data is observed from the northeast because this is a uncommon wind direction during high-pressure blocking events as seen in Figure 2. A large proportion of the data was categorized as "no specific", since the movement of the high-pressure blocking event usually results in changing wind directions.

One can observe similarities between the aerosol concentrations depending on wind directions for Vävihill and Malmö, although a larger increase can be observed in Malmö. When only considering the northeast direction, no strong increase or high levels of $\text{PM}_{2.5}$ were detected, as supported by the τ -values being under 0.5 for Malmö, and no statistically significant amount of data being found at Vävihill (Figure 9a-b). In Vävihill the southeastern direction yielded $\tau = 0.41$, however there is a clear increase until day nine, where the levels suddenly drop (Figure 9c). The τ -value for the first nine days is $\tau = 0.68$, showing a clear increase. The southeastern direction for Malmö yielded a high τ -value of $\tau = 0.64$ and mean concentration exceeding the EU annual mean limit with a maximum concentration of $26 \mu\text{g m}^{-3}$ (Figure 9d). For the western wind direction, an increase in $\text{PM}_{2.5}$ can be seen in Vävihill as supported by $\tau = 0.57$ (Figure 9e). The western wind direction for Malmö showed an increase until day eight, where it suddenly drops. Although elevated levels can be seen on day eight, one must note that the spread of the values is large (Figure 9f). The non specific direction in Figure 9g-h showed increases similar to the increase in Figure 7. This category shows that when the wind direction is changing a monotonic increase is observed, supported by $\tau = 0.70$ in Vävihill and $\tau = 0.79$ in Malmö.

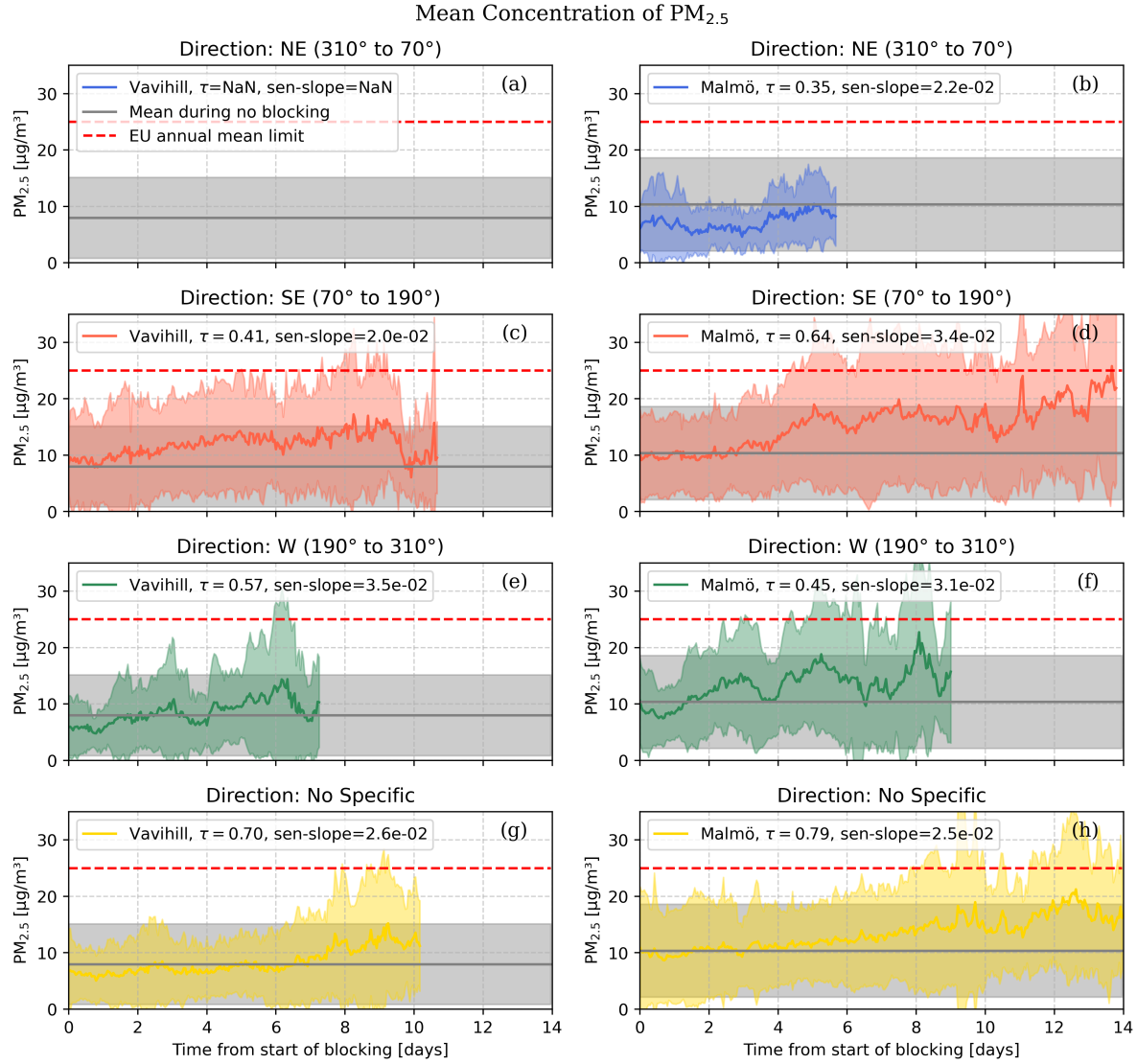


Figure 9: $\text{PM}_{2.5}$ concentrations evolution in Vävihill and Malmö for different wind directions during high-pressure blocking events. This is shown by the blue line, the mean during no high-pressure blocking event can be seen by the grey line and the EU annual mean limit is displayed by the red line. The shaded regions indicates the standard deviation of the data. Figure (a) is empty due to insufficient amount of data for the northeastern category in Vävihill.

3.1.2 The Change in Aerosol Concentrations Depending on Season

The seasonal change in concentrations of $\text{PM}_{2.5}$ during high-pressure blocking events can be seen in Figure 10. 19.8% of the events occurred during the winter, 32.8% during the spring, 19.8% during the summer and 27.6% during the autumn. From Figure 10 e-f, it is clear that the concentration during the summer for both Vävihill and Malmö does not show an increase nor high levels of $\text{PM}_{2.5}$. A slight increase can be seen for the spring in both locations, with Vävihill going from $9 \mu\text{g m}^{-3}$ to a maximum of $12 \mu\text{g m}^{-3}$, and Malmö from $11 \mu\text{g m}^{-3}$ to a maximum of $16 \mu\text{g m}^{-3}$ (Figure 10c-d). A larger increase can be seen during the autumn (Figure 10g-h), where high levels of $\text{PM}_{2.5}$ can be observed towards the end of the period, with Vävihill going from $10 \mu\text{g m}^{-3}$ to a maximum of

$16 \mu\text{g m}^{-3}$, and Malmö from $11 \mu\text{g m}^{-3}$ to a maximum of $26 \mu\text{g m}^{-3}$. During the winter, an increase in the $\text{PM}_{2.5}$ concentrations were observed, with Malmö showing a much stronger increase which is supported by $\tau = 0.70$ and the Sen's slope being $6.9 \times 10^{-2} \mu\text{g m}^{-3} \text{ d}^{-1}$ (Figure 10a-b).

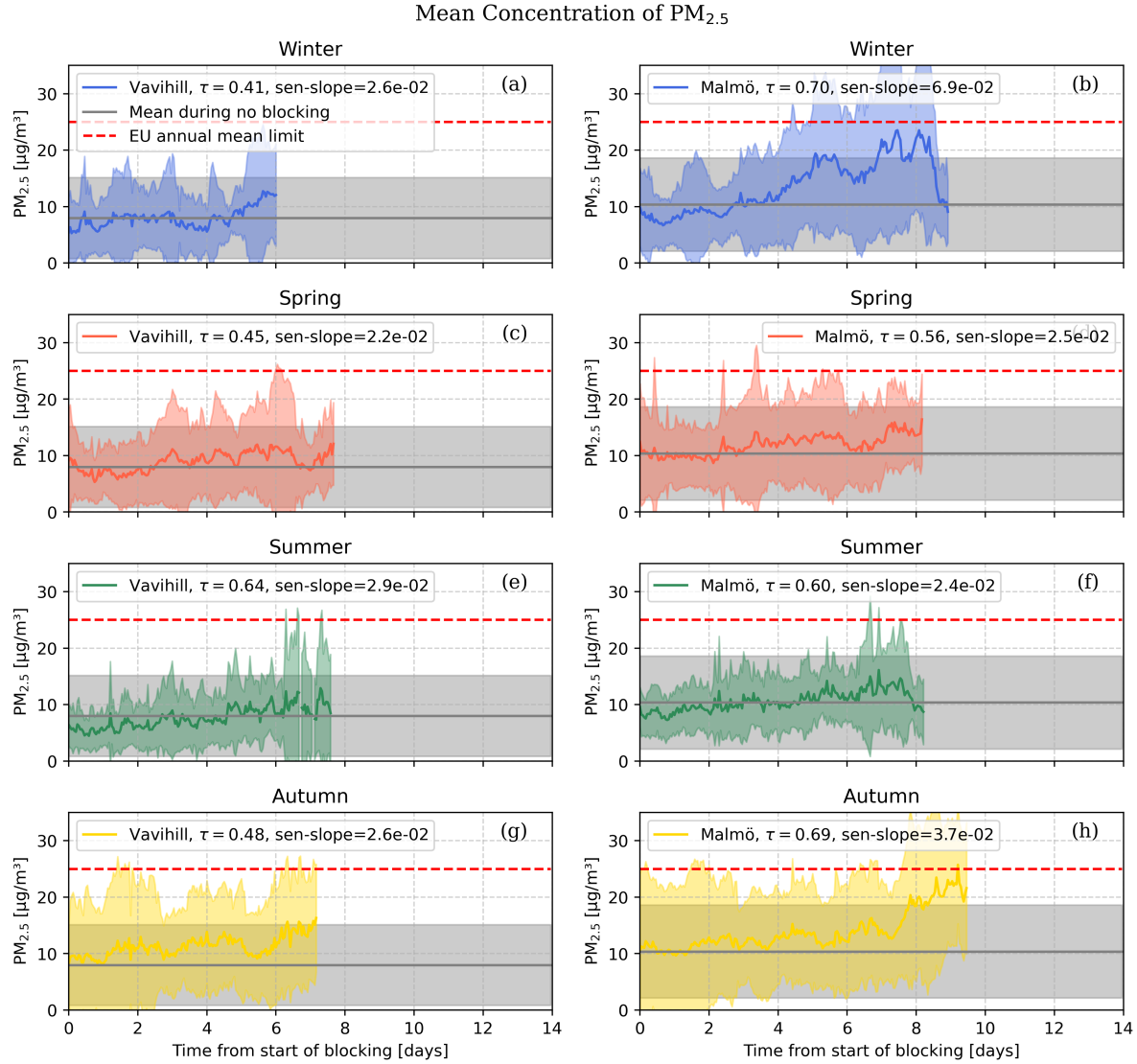


Figure 10: $\text{PM}_{2.5}$ concentrations in Vävihill and Malmö during high-pressure blocking events for different seasons. This is shown by the blue line, the mean during no high-pressure blocking event can be seen by the grey line and the EU annual mean limit is displayed by the red line. The shaded regions indicates the standard deviation of the data.

3.1.3 The Change in Aerosol Concentrations Depending on Pressure Strength

The increase in $\text{PM}_{2.5}$ concentrations depending on the strength of the high-pressure blocking event can be seen in Figure 11. In the case of Vävihill, 22.2% of the blocking events occurred with a mean pressure below 1020 hPa 45.5% occurred between 1020 and 1025 hPa and 31.3% occurred with a mean pressure over 1025hPa. In the case of Malmö, 17.0% of the blocking events occurred with a mean pressure below 1020 hPa 48.5% occurred between

1020 and 1025 hPa and 34.5% occurred with a mean pressure over 1025hPa.

From the plots, one can observe similar behaviour for the two locations. For the weaker high-pressure blocking events no prolonged increase can be seen for Malmö, nor highly elevated levels of PM_{2.5} in either location (Figure 11a-b). In the case of medium strong high-pressure blocking events a stronger increase in Vävihill $\tau = 0.62$ and weaker in Malmö $\tau = 0.30$ can be seen. When observing both plots one can see a maximum around day nine, although the maximum in Malmö has a larger value spread (Figure 11c-d). For the stronger high-pressure blocking events one can see a strong increase in the case of Malmö and in Vävihill, although the increase in Vävihill is slightly weaker. When viewing the plots Figure 11e-f one observes that the levels of PM_{2.5} in the case of Vävihill and Malmö exceed the normal range at day thirteen, where the mean reached the EU annual mean limit for Malmö. In Vävihill the values went from 9 $\mu\text{g m}^{-3}$ to a maximum of 21 $\mu\text{g m}^{-3}$, and in Malmö they went from 12 $\mu\text{g m}^{-3}$ to a maximum of 28 $\mu\text{g m}^{-3}$.

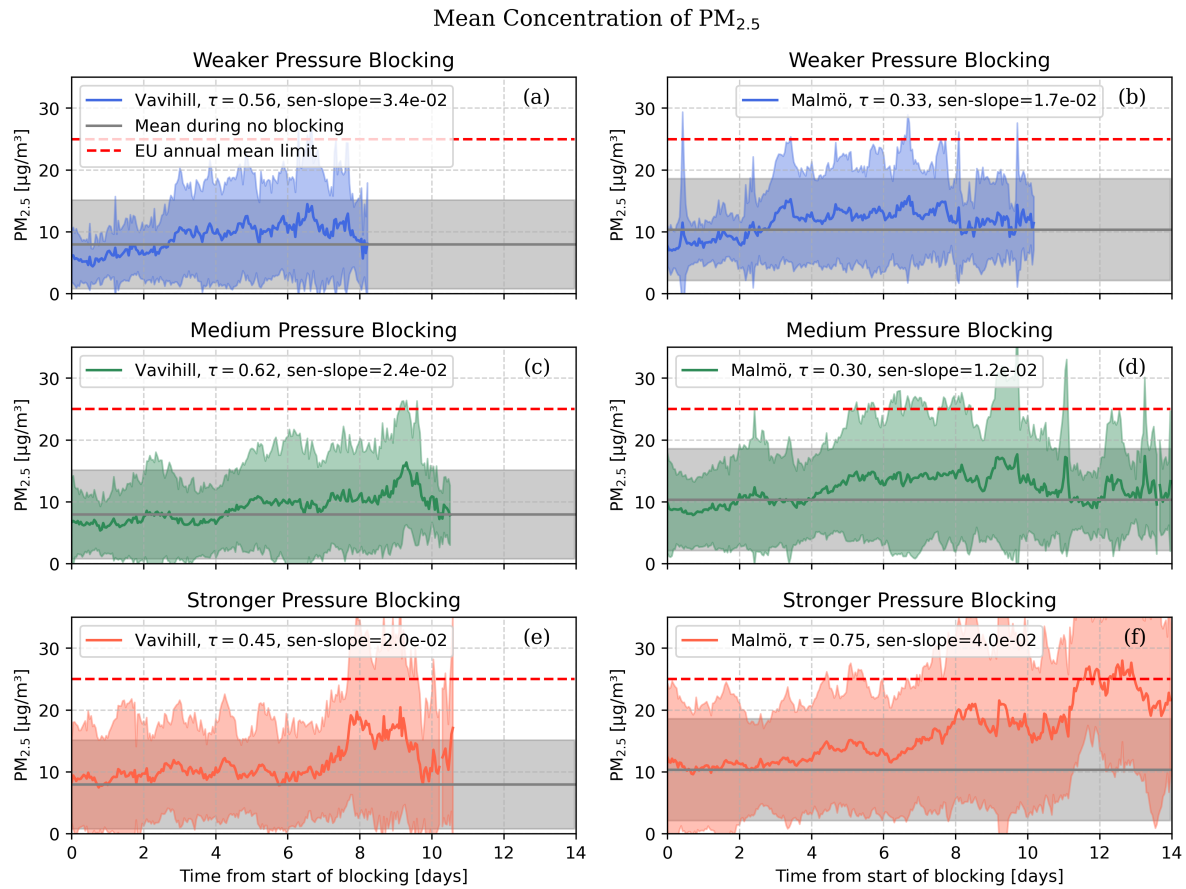


Figure 11: PM_{2.5} concentrations in Vävihill and Malmö for different pressure strengths during high-pressure blocking events. This is shown by the blue line, the mean during no high-pressure blocking event can be seen by the grey line and the EU annual mean limit is displayed by the red line. The shaded regions indicates the standard deviation of the data.

Figure 7–11 all had a p-value, from the Mann-Kendall test, of their respectively increase approximately equal to 0, providing significant results. From Figure 7–11 it is clear that the high elevations of PM_{2.5} occur after eight to

thirteen days. These results indicates that prolonged periods of high-pressure blocking events indicate an accumulative increase of PM_{2.5}, which can be seen in Figure 7 where one can see that the combination of all the other plots resulted in a steady increase in the case of Malmö, and an increase in the case of Vavihill. The only case where no increase is observed is when the wind direction is from the northeast (see Figure 9 a-b), which is not very common. This result indicates that for high-pressure blocking events one observes an increase in the concentration of PM_{2.5} after eight to thirteen days regardless of the type of high-pressure blocking event, even though different types of high-pressure blocking events may differ in their specific increase. Especially strong increases with elevated PM_{2.5} levels could be seen with winds from the southeast and for stronger high-pressure blocking events.

3.2 The Frequency of High-Pressure Blocking Events

The last task was to determine whether high-pressure blocking events have become more common. When observing the number of high-pressure blocking events per year, no significant change in frequency could be seen (see Figure 12). Since the highest levels of PM_{2.5} occurred toward the end of the events (see Figure 7–11), the frequency of longer high-pressure blocking events was also examined. However, no increase could be observed in any of the cases. More interestingly, a small decrease can be observed from the τ -values and the Sen's slope values. However, one must note that the p-values, from the Mann-Kendall test, are much larger here than Figure 7–11.

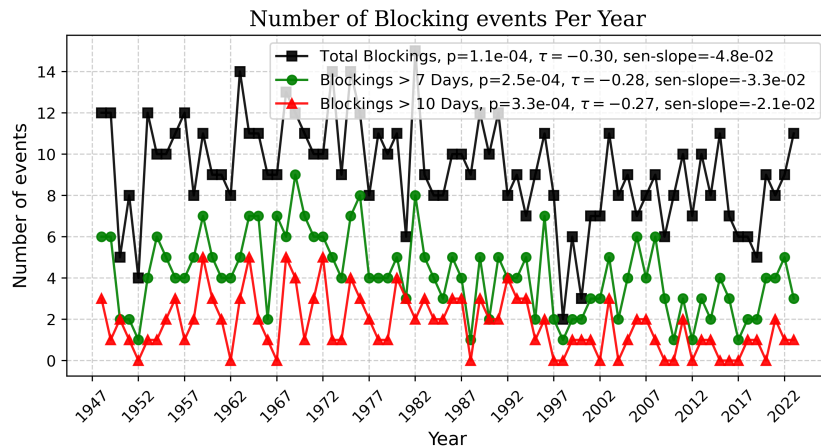


Figure 12: fig: This plot show the change in frequency of high-pressure blocking events. The plots also indicates the change in events longer than seven and ten days.

In Figure 13, the number of days with high-pressure blocking events per year can be seen. Here, the total, seasonal, and pressure strength dependence can be observed. The reason for not including the directional dependence is that no wind data was available for this period. Even here a slight decrease can be seen in most plots, especially the total blocking days per year (h).

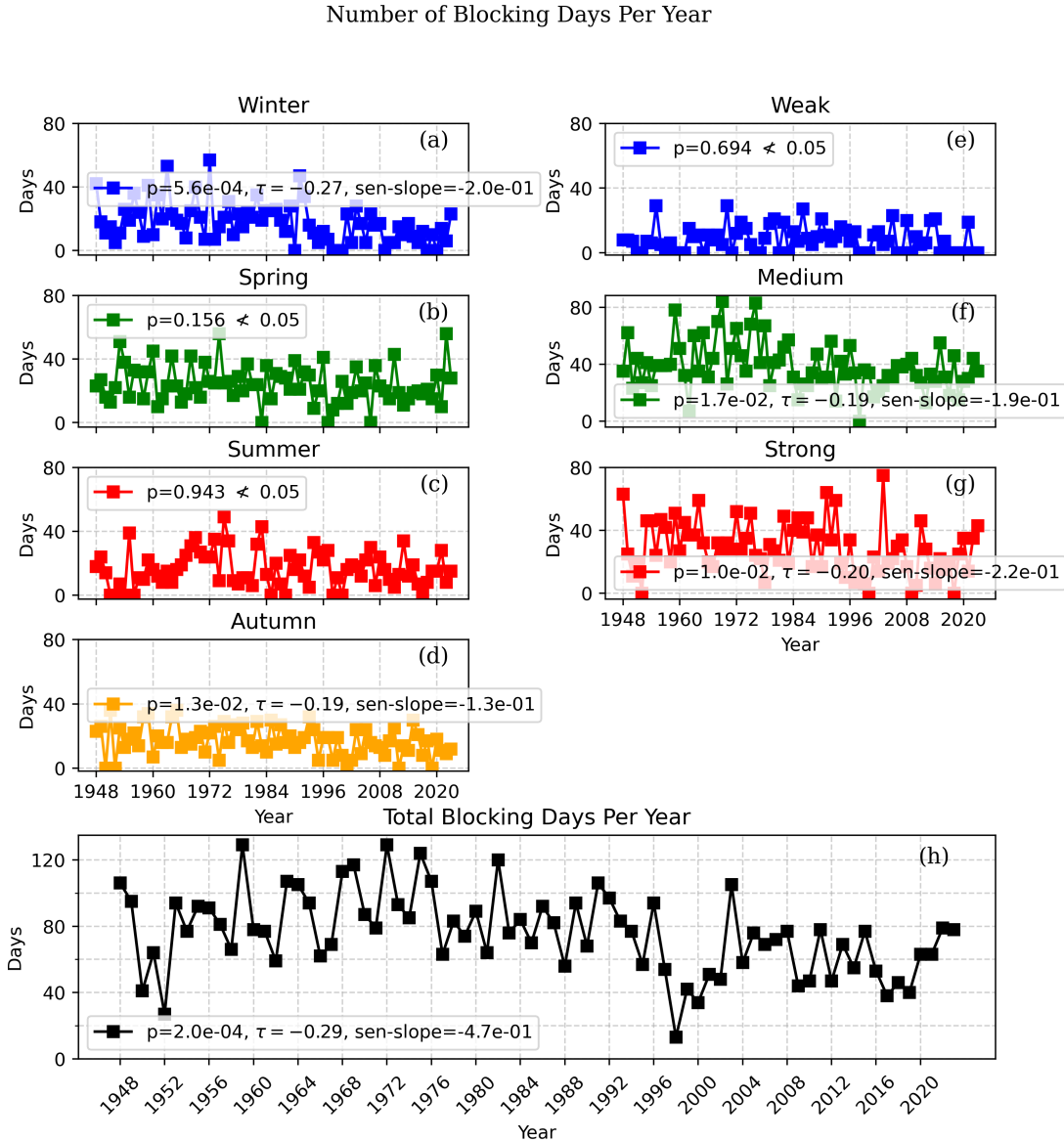


Figure 13: The number of days under a high-pressure blocking event each year, during each season, and for different pressure strengths. If the p -value was greater than 0.05, the corresponding τ -value and Sen's slope were discarded, as the test was deemed statistically insignificant.

When observing the slight decline of the frequency of the high-pressure blocking events in Figure 12 and Figure 13 one must note that the low $|\tau|$ -values indicate that the trend is not monotonic. Furthermore, the large p -values in Figure 13 indicate that the trend is more random in comparison to the mean aerosol concentration plots observed in Figures 7–11. One can observe that no type of high-pressure blocking events has become more common during the last 74 years. This is an interesting result since this aligns with the observations from other studies, where a decline of high-pressure blocking events has been observed during the late 20th century [3].

4 Discussion

The result above showed that for all high-pressure blocking events, except for events with winds from the northeast, an aerosol increase was seen after eight to thirteen days compared to the initial aerosol values. This outcome provides an important result, which is that the aerosol concentration accumulates during high-pressure blocking events. An interesting observation is that this occurs after this specific time. However, it was also observed that when the high-pressure blocking event disappeared, the aerosol levels returned to normal within a day.

One important concept to discuss is whether the accumulation of aerosol is due to local emissions or particle advection from other locations. To address this question, several observations can be made: Firstly, local emissions in urban Malmö should be much higher than those in rural Vavihill, if the increase is due to local emissions. Secondly, if the increase is due to particle advection, the increase should depend strongly on the wind direction.

From all the plots regarding PM_{2.5}, one can observe that the increase in Malmö is generally stronger than in Vavihill. This suggests, as predicted, that some of the increase in aerosol is due to local emissions. One could argue that this increase might be due to other factors, such as the fact that Malmö is coastal, whereas Vavihill is not, or that Malmö is located near regions with higher emissions, such as central Europe. However, this is unlikely to be the case. Firstly, the fact that Malmö is coastal would not suggest a higher aerosol increase than in Vavihill. The coastal factor may influence the overall air quality in the location, but since we are observing local changes, this factor should be accounted for. The argument that Malmö is more closely located to central Europe, especially in the southeastern direction may play a role in the stronger increase in Malmö than Vavihill. This is due to the fact that stronger high-pressure blocking events indicate more stagnant air which would imply that locations closer to the locations of high emission would be impacted more strongly than locations further away. However, the length scale to central Europe compared to the length scale between Vavihill and Malmö makes this factor negligible. Furthermore, other large urban areas such as Copenhagen are not substantially closer to Malmö than Vavihill.

If we examine the wind dependence, we observe another interesting result. For wind directions from the northeast, there is no noticeable increase in aerosols in Malmö, whereas we see a stronger increase when the wind comes from the west, and an even stronger increase from the southeastern direction. This suggests that some of the particle increase is due to particle advection. One could argue that this directional increase has more to do with the different types of high-pressure blocking events. However, the main difference between different types of high-pressure blocking events is where they are centred, which mainly correspond to different wind directions. The non-specified wind direction showed a monotone increase for both locations; however, this increase is not as strong as the increase observed for the southeastern direction for Malmö and for Vavihill, if one observes the initial eight days. Furthermore, the northeast direction in Malmö showed a smaller increase than the non-specified direction. This would suggest that the wind from the northeast contains cleaner air, whereas the wind from the southeast is exhibiting a higher aerosol concentration.

Another important concept to discuss is the difference in the aerosol increase between the rural and urban location. In the plots above one could observe that the aerosol accumulation was stronger in the case for the urban location in comparison to the rural. Several reasons could explain this behaviour. Firstly, emissions in the urban location should be higher than in the case of the rural location. This is supported by the seasonal dependence where similar behaviour of the aerosol concentrations is seen for both locations except during the winter, where a larger increase is seen in the urban location. Since aerosols emissions increase due to road transportation with winter tyres and worse road surfaces one would expect a stronger increase in the urban location during the winter.

However, the aerosol advection from nearby countries should also be increased during the winter. In southern Sweden district heating is the most common type of domestic heating, whereas countries to the southeast and east, such as Poland, use more heat produced by coal combustion. The process of coal combustion for domestic heating produces considerable amounts of aerosols, which could be dispersed or advected to southern Sweden. However, the observation that aerosol concentrations are much higher in Malmö than in Vavihill during winter suggests that advection from nearby countries does not explain the entire picture.

Another reason might be the difference in the inversion layer for the different locations. Although the natural description of the two locations are similar, the skyline due to buildings is not. The urban location has many buildings which hold moisture badly, whereas the rural is characterised by nearby trees and hills which are better at holding moisture. This makes the ground more dependent on the ground radiation, which results in a clearer ground inversion layer in the urban location. One would thus obtain more vertical air mixture in the rural location, which would contribute to the lower levels of aerosols in this location.

Since the aerosol levels mainly differ during the winter, one could argue that the main difference between the rural and the urban location is the local emissions. However, one could note that the ground inversion during the winter is amplified due to longer nights, which would amplify the inversion layer and prevent further air mixing (just like the ground inversion during the summer should be limited). Even though the inversion is mainly affected by the subsidence inversion, which is similar for the two locations, the ground inversion should still affect the total inversion. One could thus conclude that the total inversion is increased during the winter due to the ground inversion amplifying the total inversion in both locations. The slightly stronger ground inversion in the urban location together with the larger emissions of the urban location would give a higher aerosol concentration.

5 Conclusion and Summary

This thesis has demonstrated that the presence of high-pressure blocking events in southern Sweden significantly increased the aerosol concentration in both rural and urban locations. The mean PM_{2.5} in Malmö went from 10 µg m⁻³ to a maximum of 21 µg m⁻³ during the high-pressure blocking event, and an increase from 7 µg m⁻³ to a maximum of 18 µg m⁻³ could be observed in Vavihill during the event. Increased levels of PM_{2.5} were seen in both locations after eight to thirteen days of uninterrupted high-pressure blocking, indicating accumulation of aerosols during the events. This accumulation was mainly attributed to the presence of a subsidence inversion layer, which prohibits vertical air mixing. However, it was also observed that once the high-pressure blocking event subsided, aerosol levels returned to normal within a day. A stronger increase was found in the urban area of Malmö than the rural area of Vavihill, which was mainly attributed to local emissions and a slightly stronger ground inversion, especially during the winter. The wind directional dependence on PM_{2.5} concentrations indicated that the long-range advection of aerosols was a significant contributor to aerosol concentration in the region, where winds from central and eastern Europe significantly increased the aerosol levels. The seasonal dependence indicated an increase during the winter. A stronger increase was also observed with stronger high-pressure blocking events, where the highest levels of PM_{2.5} could be observed. Observing the lengths and number of high-pressure blocking events showed that there has not been an increase of any sort during the last 74 years, which aligns with other European studies.

To summarize, the analysis of aerosol concentrations during meteorological events is important for monitoring the health risks associated with different meteorological phenomena. This thesis has shown that not only domestic emissions play a role in air quality, but that advection from nearby countries also plays a crucial role. This shows the magnitude of international work to prohibit the large-scale emissions of aerosols. As the climate changes, so does the weather, and understanding how these changes affect us is of utmost importance.

6 Outlook

Future work on this subject should use a more advanced classification of different types of high-pressure blocking events by using data from multiple meteorological stations. This would create a clearer view of the actual movement of the anticyclone, which could be used to simulate the advection of aerosols. Comparing this simulation with the values from this thesis would give more insight into the actual advection of the aerosols. To study local emissions, one could monitor the local emission and compare this to the aerosol concentrations during high-pressure blocking events to see the effect that these play. To analyse the role of the inversion layer during the event, one could monitor vertical atmospheric data to see the effect of the subsidence inversion on the aerosol concentrations.

References

- [1] NASA. Haze over Europe. <https://earthobservatory.nasa.gov/images/11219/haze-over-europe>, March 2003.
- [2] John F. B. Mitchell, Jason Lowe, Richard A. Wood, and Michael Vellinga. Extreme events due to human-induced climate change. *Philosophical Transactions of the Royal Society A: Mathematical, Physical and Engineering Sciences*, 364(1845):2117–2133, 2006.
- [3] Anthony R. Lupo. Atmospheric blocking events: A review. <https://doi.org/10.1111/nyas.14557>, December 2020.
- [4] Wenyue Cai, Xiangde Xu, Xinghong Cheng, Fengying Wei, Xinfia Qiu, and Wenhui Zhu. Impact of “blocking” structure in the troposphere on the wintertime persistent heavy air pollution in northern China. *Science of The Total Environment*, 741:140325, 2020.
- [5] Vlado Spiridonov and Ćurić Mladjen. Cyclones and Anticyclones | SpringerLink. https://link.springer.com/chapter/10.1007/978-3-030-52655-9_17, November 2020.
- [6] E. Gramsch, D. Cáceres, P. Oyola, F. Reyes, Y. Vásquez, M. A. Rubio, and G. Sánchez. Influence of surface and subsidence thermal inversion on PM2.5 and black carbon concentration. *Atmospheric Environment*, 98:290–298, December 2014.
- [7] Formation of Subsidence Inversions. *Thomson Higher Education.*, 2007.
- [8] Greg O’Hare, Rob Wilby, and John Sweeney and Rob Wilby. *Weather, Climate and Climate Change*. Pearson Eductaion Limited, England, 2005.
- [9] Magdalena Porębska and Małgorzata Zdunek. Analysis of extreme temperature events in Central Europe related to high pressure blocking situations in 2001–2011. *Meteorologische Zeitschrift*, 22(5):533–540, 2013.
- [10] Judit Bartholy, Rita Pongracz, and Margit Pattantyús-Ábrahám. European Cyclone Track Analysis Based on ECMWF ERA-40 Data Sets. *International Journal of Climatology*, 26(11):1517–1527, 2006.
- [11] Noelia Otero, Oscar E. Jurado, Tim Butler, and Henning W. Rust. The impact of atmospheric blocking on the compounding effect of ozone pollution and temperature: A copula-based approach. *Atmospheric Chemistry and Physics*, 22(3):1905–1919, 2022.
- [12] Sigler, Marian. Blank map of Europe (with disputed regions). [https://commons.wikimedia.org/wiki/File:Blank_map_of_Europe_\(with_disputed_regions\).svg](https://commons.wikimedia.org/wiki/File:Blank_map_of_Europe_(with_disputed_regions).svg), February 2007.
- [13] European Environment Agency. Europe’s air quality status 2024. <https://www.eea.europa.eu/publications/europe-s-air-quality-status-2024>, 2024.
- [14] Shubham Sharma, Mina Chandra, and Sri Harsha Kota. Health Effects Associated with PM2.5: A Systematic Review. *Current Pollution Reports*, 6(4):345–367, 2020.

- [15] Ulla Arthur Hvidtfeldt, Mette Sørensen, Camilla Geels, Matthias Ketzel, Jibran Khan, Anne Tjønneland, Kim Overvad, Jørgen Brandt, and Ole Raaschou-Nielsen. Long-term residential exposure to PM_{2.5}, PM₁₀, black carbon, NO₂, and ozone and mortality in a Danish cohort. *Environment International*, 123:265–272, February 2019.
- [16] A. Analitis, P. Michelozzi, D. D’Ippoliti, F. De’Donato, B. Menne, F. Matthies, R. W. Atkinson, C. Iñiguez, X. Basagaña, A. Schneider, A. Lefranc, A. Paldy, L. Bisanti, and K. Katsouyanni. Effects of heat waves on mortality: Effect modification and confounding by air pollutants. *Epidemiology*, 25(1):15–22, 2014.
- [17] Thermo Fisher Scientific Inc. TEOM® Series 1400a Ambient Particulate (PM-10) Monitor Operating Manual, 2007.
- [18] PALAS GmbH. Operating Manual: Fidas® Fine Dust Monitor System.
- [19] Thermo Scientific. 8500 FDMS Filter Dynamics Measurement System, 2010.
- [20] S. Persson. Autumn colors in Söderåsen National Park.
- [21] J. Jönsson (Julle). Södervärn bus station, Malmö, Sweden, April 2015.
- [22] E. Frohne. Location map of Skåne County in Sweden, January 2009.
- [23] VAISALA. PTB 200 DIGITAL BAROMETERS USER’S GUIDE, February 1993.
- [24] VAISALA. PTB220 Series Digital Barometers USER’S GUIDE, August 2001.
- [25] VAISALA. Wind Set WA15 and WA25. <https://www.vaisala.com/en/products/weather-environmental-sensors/wind-set-wa15>, January 2021.
- [26] GEONOR, Inc. T-200B Series All Weather Gauge. <https://www.geonor.com/t-200b-all-weather-precipitation—rain-gauge>, 2019.
- [27] Hussain, Md. and Mahmud, Ishtiaq. pyMannKendall: A python package for non parametric Mann Kendall family of trend tests. *Journal of Open Source Software*, 4(3):1556, July 2019.

A Appendix: Access to Code

The full source code, data files, and LaTeX source for this thesis are available on GitHub at:

<https://github.com/FredrikBergelv/BachelorThesis>

The repository includes all Python scripts used for data processing, statistical analysis, and figure generation, as well as the LaTeX files used to compile this document. Please refer to the ‘README.md’ file in the repository for an overview of the file structure and dependencies. The code is licensed for academic use, and citation of the work is appreciated.